Nonlinear Dyn (2020) 100:1809–1824
https://doi.org/10.1007/s11071-020-05576-9

ORIGINAL PAPER

Different synaptic connections evoke different firing patterns in neurons subject to an electromagnetic field

Nazanin Zandi-Mehran · Sajad Jafari · Seyed Mohammad Reza Hashemi Golpayegani · Fahimeh Nazarimehr · Matjaž Perc

Received: 9 October 2019 / Accepted: 13 March 2020 / Published online: 30 March 2020

Abstract The electrical activity of neurons depends on the physiological conditions in the nervous system. An electromagnetic field, for example, can significantly affect the dynamics of individual neural cells, and it also affects their collective dynamics. It is therefore of interest to study the neuronal dynamics under such an influence in various setups. We thus study the firing patterns in two coupled neurons by considering three different types of synapses, namely electrical, chemical, and electrochemical. We use the Hindmarsh–Rose mathematical model as the basis of neuronal dynamics, and we also introduce an electromagnetic field effect. We conduct extensive calculations of the firing patterns, and we determine the bifurcation diagrams for constant and periodic external currents. The results show that the different synaptic connections evoke different firing patterns and that in general electrochemical synapses can show richer variety of dynamical behavior than electrical or chemical synapses.

Keywords Hindmarsh–Rose model · Coupling · Electromagnetic field · Electrical coupling · Chemical coupling · Mixed coupling

N. Zandi-Mehran · S. Jafari (✉) ·
S. M. R. Hashemi Golpayegani · F. Nazarimehr
Biomedical Engineering Department, Amirkabir University of Technology, Tehran 15875-4413, Iran
e-mail: sajadjafari83@gmail.com

N. Zandi-Mehran
e-mail: nazaninznd@yahoo.com

S. M. R. Hashemi Golpayegani
e-mail: mrhashemigolpayegani@gmail.com

F. Nazarimehr
e-mail: fahimenazarimehr@gmail.com

Matjaž Perc
Faculty of Natural Sciences and Mathematics, University of Maribor, Koroška cesta 160, 2000 Maribor, Slovenia

Matjaž Perc
Department of Medical Research, China Medical University Hospital, China Medical University, Taichung, Taiwan

Matjaž Perc
Complexity Science Hub Vienna, Josefstädterstraße 39, 1080 Vienna, Austria
e-mail: matjaz.perc@gmail.com

1 Introduction

Brain structure and its functions have been studied extensively for many years. The nervous system contains billions of various neurons which play different roles [1]. Biomedical researchers and neurologists have established that the neurons are elementary units for processing the information, mainly through burst behaviors [2,3]. However, there are rare types of neurons that are non-spiking [4]. Neurons communicate with each other through the small gap between the axon of the sender and dendrites of the receiver [5]. This gap is called the synapse, the sender neuron is called presynaptic, and the receiver is called postsynaptic [5].

There are different types of synapses [6,7]. The most typical synapse of the vertebrate is the chem-

ical synapse [8]. In the chemical synapse, when the spikes reach the terminal land (through the axon of the presynaptic neuron), the voltage-sensitive calcium channels are opened near the end of the neuron. Then, the calcium flows into the neuron that leads the vesicles of neurotransmitters to release from the presynaptic neuron in the synapse. By spreading the neurotransmitters over the synaptic cleft (in the scale of 20nm), ligand-gated ion channels are activated [8]. Depending on the involved ions and neurotransmitters, the postsynaptic neuron is excited or inhibited [9]. In an electrical synapse, the neighboring neurons are connected with channels that create directed paths. These channels transform the ions and small molecules through the gap junction [10,11]. Researches have shown that the electrochemical synapses or "mixed" synapses also exist in the central nervous system of mammalians or even rodents [12–14]. By modeling the neurons, an insight into terminals is achieved, and the connections are investigated.

In the modeling of the neurons, a mathematical structure is selected in the first step. Then, based on the desired aspects of a neuron dynamic, the model is evolved [15]. A basic neural model is Hodgkin–Huxley (HH), which describes the time evolution of the membrane potential [16]. Since the HH model is very complicated, its equations have been modified by other researchers to obtain simpler models. FitzHugh–Nagumo, Izhikevich, and Hindmarsh–Rose are some of such models [17–20]. The Hindmarsh–Rose model can represent many types of neuron's dynamics [21,22]. A modification of this model has been proposed to consider the influence of the electromagnetic field [23]. The electromagnetic field effect has been added to the model with the extension of the ODE system. In the neural cells, during variations of the flow of ions in the cell, the inner distribution density of ions becomes time-varying to trigger electric and magnetic fields. The field distribution is enhanced when more neurons are involved in the space. The magnetic flux can be simulated by memristive memory conductance [24]. The effect of adaption current on membrane potential with a time delay has been studied in [25].

To better understand the neuronal behavior and the transmission of information, the study of the neuronal coupling is essential [26]. Researches have shown that the brain contains, on average, 86.1 ± 8.1 billion neurons, and each neuron has many connections [27]. By some estimates, over 100 trillion synapses exist [28]. It is essential to investigate the dynamical behavior of coupled neurons, beside analysis of a single neuron. To this aim, the simplest structure is two coupled neurons. Studying the coupling of neurons under the electromagnetic field is of interest [29]. By increasing the coupling intensity, synchronization rhythm can be seen [30]. The effect of chemical and electrical synapses in the synchronization rhythm was discussed in [31]. Spiral waves of a square array network of Hindmarsh–Rose neurons with nearest-neighbor connections and under magnetic fields were studied [32]. The effect of the distribution of the electromagnetic field in a chain network has been investigated and showed that coupling in the field could affect signal communication [33]. Reference [34] has shown that in the coupling of two neurons with magnetic flux coupling, perfect phase synchronization can be induced. It has shown that in a larger current force, the phase synchronization threshold is increased.

In this paper, the impact of three electrical, chemical, and electrochemical couplings is studied on the two coupled Hindmarsh–Rose neurons under magnetic field effects. Such study is essential because firstly, in real world the neurons are working together. So it is crucial to investigate the dynamics of coupled neurons. Secondly, the neurons are in connection via magnetic fields besides chemical and electrical connections. In Sect. 2 of the paper, the Hindmarsh–Rose model and its modification under the magnetic field are studied. Dynamical properties of this model are discussed in this section. Electrical, chemical, and electrochemical couplings of the two coupled neurons are investigated in Sect. 3. Finally, the paper is concluded in Sect. 4.

2 The neural model under magnetic flow

In 1982, Hindmarsh and Rose proposed a neuron model which can represent a variety of rich dynamical solutions [35]. At first, this model was described as a two-dimensional ordinary differential equation that could not represent burst or chaotic dynamics [20]. So, a third equation was added to the Hindmarsh–Rose (HR) system [24]. This variable shows a slow dynamic in a linear form, referring to the hyperpolarization current. The latest set of equations is given by

$$\begin{aligned} \dot{x} &= y - ax^3 + bx^2 - z + I_{\text{ext}} \\ \dot{y} &= c - dx^2 - y \\ \dot{z} &= r[s(x - x_0) - z] \end{aligned} \tag{1}$$

where x, y, and z are membrane potential, recovery variable (or spiking variable), and bursting variable, respectively. I_{ext} represents the external current or clamping current. Four parameters, a, b, c, and d, are positive constants, usually set to $a = 1$, $b = 3$, $c = 1$, and $d = 5$ [24]. The third equation was added to show the neural dynamics better. In this equation, x_0 is the resting potential of the neuron and the parameters r and s are positive constants with $r \ll 1$ [36]. Also, z was added to the first equation to show the effect of the slow current on the membrane potential [22].

To investigate the effect of the electromagnetic radiation, an improved version of the HR neuron was proposed [37]. Using the structure of HR model (Eq. 1), a four-dimensional model was proposed to represent the electromagnetic induction effect [38]. The modified model is as follows:

$$\begin{aligned} \mathrm{d}x/\mathrm{d}t &= y - ax^3 + bx^2 - z + I_{\text{ext}} - k_1\rho(\varphi)x \\ \mathrm{d}y/\mathrm{d}t &= c - dx^2 - y \\ \mathrm{d}z/\mathrm{d}t &= r[s(x - x_0) - z] \\ \mathrm{d}\varphi/\mathrm{d}t &= kx - k_2\varphi \end{aligned} \tag{2}$$

where the new variable φ is magnetic flux across the membrane of the neuron. Its derivation is computed by the difference of the membrane potential and leakage of magnetic flux [23,39]. The rate of change of electric charge to the magnetic flux ($\mathrm{d}q(\varphi)/\mathrm{d}\varphi$) is defined by $\rho(\varphi)$, that is, a memristive memory conductance (memductance). $\rho(\varphi)$ is an ideal memristor obtained by $\rho(\varphi) = \alpha + 3\beta\varphi^2$, where α, β are constant parameters as $\alpha = 0.1$, $\beta = 0.02$ [40]. Justification of the last term of x in Eq. 2 can be described by the third Maxwell's equation (Faraday's law), a changing magnetic field causes an electrical field, while the direction is given by the Lenz's law [41]. Also, inner propagation and changing charged ions in channels can induce magnetic and electric fields [42]. Figure 1 shows the magnetic field around a neuron. The generated current intensity can be computed by the rate of changes in electrical charges over time. Using derived chain rule, $\mathrm{d}q/\mathrm{d}t$ can be obtained by multiplication of $\mathrm{d}q(\varphi)/\mathrm{d}\varphi$ by $\mathrm{d}\varphi/\mathrm{d}t$. $\mathrm{d}q(\varphi)/\mathrm{d}\varphi$ and $\mathrm{d}\varphi/\mathrm{d}t$ are $\rho(\varphi)$ and electromotive force, respectively. The electromotive force is defined as a proportion of voltage variable x. $k_1\rho(\varphi)x$ is the feedback term that should be subtracted [43]. System parameters are constant as $x_0 = -1.6$, $r = 0.006$, $k = 1$, $s = 4$. As mentioned above, k_1 and k_2 denote the interaction between magnetic flux and membrane potential, which can be used as bifurcation parameters.

The bifurcation diagram of the neuron of Eq. 2 concerning the external current force is shown in Fig. 2. There are two methods to plot the bifurcation diagram: inter-spike intervals (ISIs) and peak detection. ISIs of the membrane potential convey the information of the encoding of the time series [44]. Figure 2a shows the ISIs of the neuron in different external currents, and Fig. 2b represents the peaks of the membrane potential.

In Fig. 2a, by increasing the external current, a lower branch of ISIs is produced, and these two different branches of ISIs are converged together in larger parameters. A higher branch of ISIs without any lower branch shows spike behavior for I_{ext} in the interval [2, 2.4]. The creation of the lower branch after $I_{\text{ext}} = 2.4$ illustrates a typical bursting dynamic. After that, the chaotic dynamics emerge. Finally in higher values of parameter, fast-spiking is observed. Similarly, the chaotic regime exists in Fig. 2b. By increasing the external current, the peak values are increased. In parameter, approximately equal to 3.8 consecutive spikes with uniformly decreasing peak values can be seen. In Fig. 3, the dynamics of neurons in four different external currents are plotted. In smaller values of the external current force, an initial burst can be observed (Fig. 3a). By increasing the current force, spikes with longer time intervals are formed (Fig. 3b). Afterward, the chaotic burst dynamics are created (Fig. 3c). In Fig. 3d, fast-spiking dynamics are seen.

In the neural cells, during variations of the flow of ions in the cell, the inner distribution density of ions becomes time-varying to trigger electric and magnetic fields. In fact, outside of each cell, electric and magnetic fields exist similar to the inside. The field distribution is enhanced when more neurons are involved in the space. This model emphasizes the contribution of the inner magnetic field, and the effect of the electric field is left out. Also, when external forcing is applied, the excitability is changed. Thus, the inner field distribution is also changed; even the external current force can induce a magnetic field by itself. However, the effect of external forcing on the magnetic field can be considered in the adjustment of the coefficients for the current force. The magnetic field is induced by the flow of ions in the cell, while membrane potential is adjusted in the same [42]. In this model, the magnetic field is considered an inner field of the cell. This kind of magnetic field seldom shows periodicity because of its complexity in the flow of charged ions.

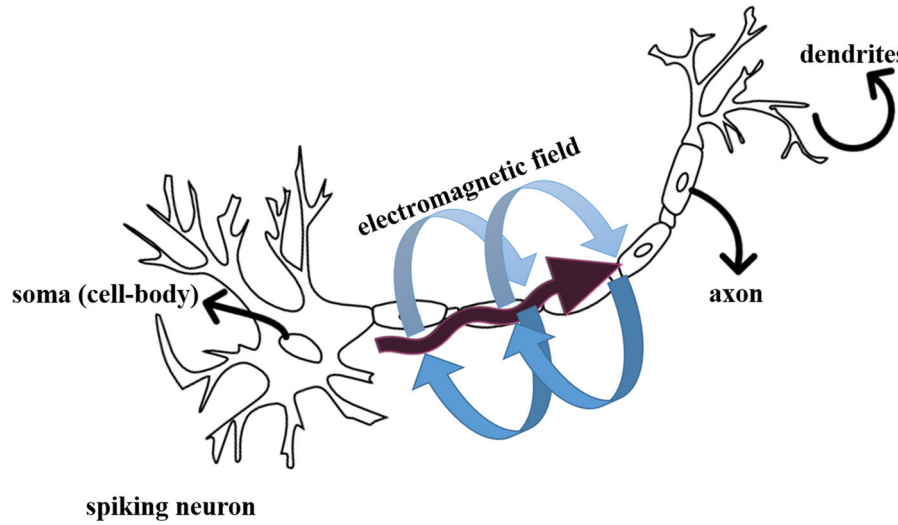

Fig. 1 Neuron under an electromagnetic field

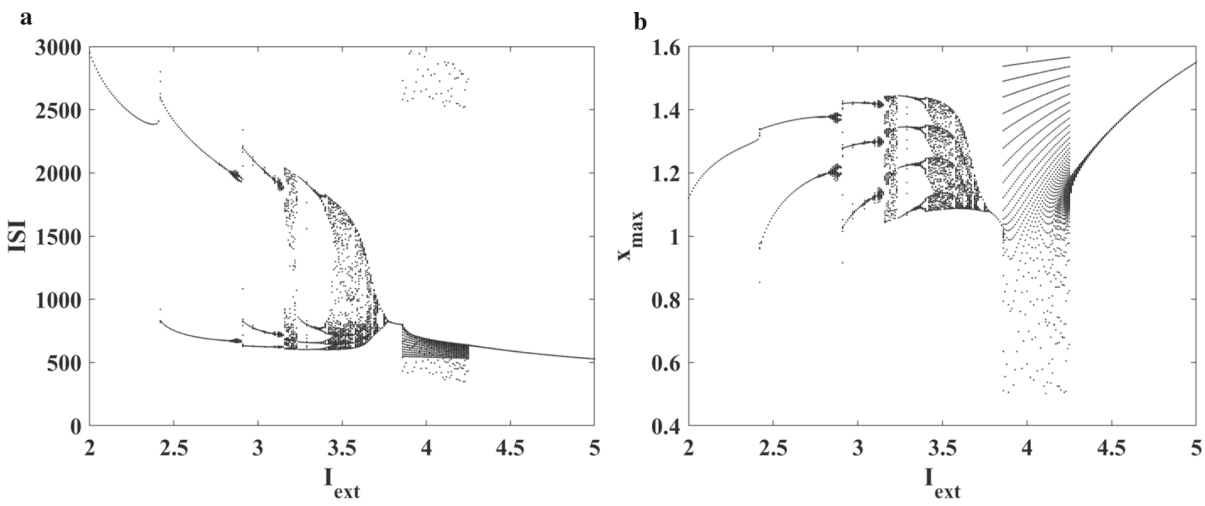

Fig. 2 Bifurcation diagram of the modified HR neuron (Eq. 2) by using constant initial conditions $(0.2, 0.5, 0.1, 0.1)$. **a** ISIs with respect to external current force (I_{ext}); **b** peak values with respect to external current force (I_{ext}); the parameters are $a = 1, b = 3, c = 1, d = 5, k = 1, r = 0.006, s = 4, k_1 = 1, k_2 = 0.5, \alpha = 0.1, \beta = 0.02$

3 Coupling of two neurons

In this section, the dynamics of two coupled neurons are considered. In the following, three main types of connections are studied: electrical, chemical, and electrochemical couplings. In each subsection, a short physiological review is presented, and the neural dynamics are investigated.

3.1 Electrical coupling

Most of the studies focusing on the coupling of neurons have been performed based on the coupling between the membrane voltages [45–50]. The effect of each neuron on the others can be modeled by a simple feedback term, representing its voltage. In other words, membrane voltages are connected directly like a wire [49]. The electrical coupling is one type of transmissions which causes the ions to transmit directly from a gap junction [51]. In these couplings, the voltage spreads to the other cells [45]. To show these effects, a proportion

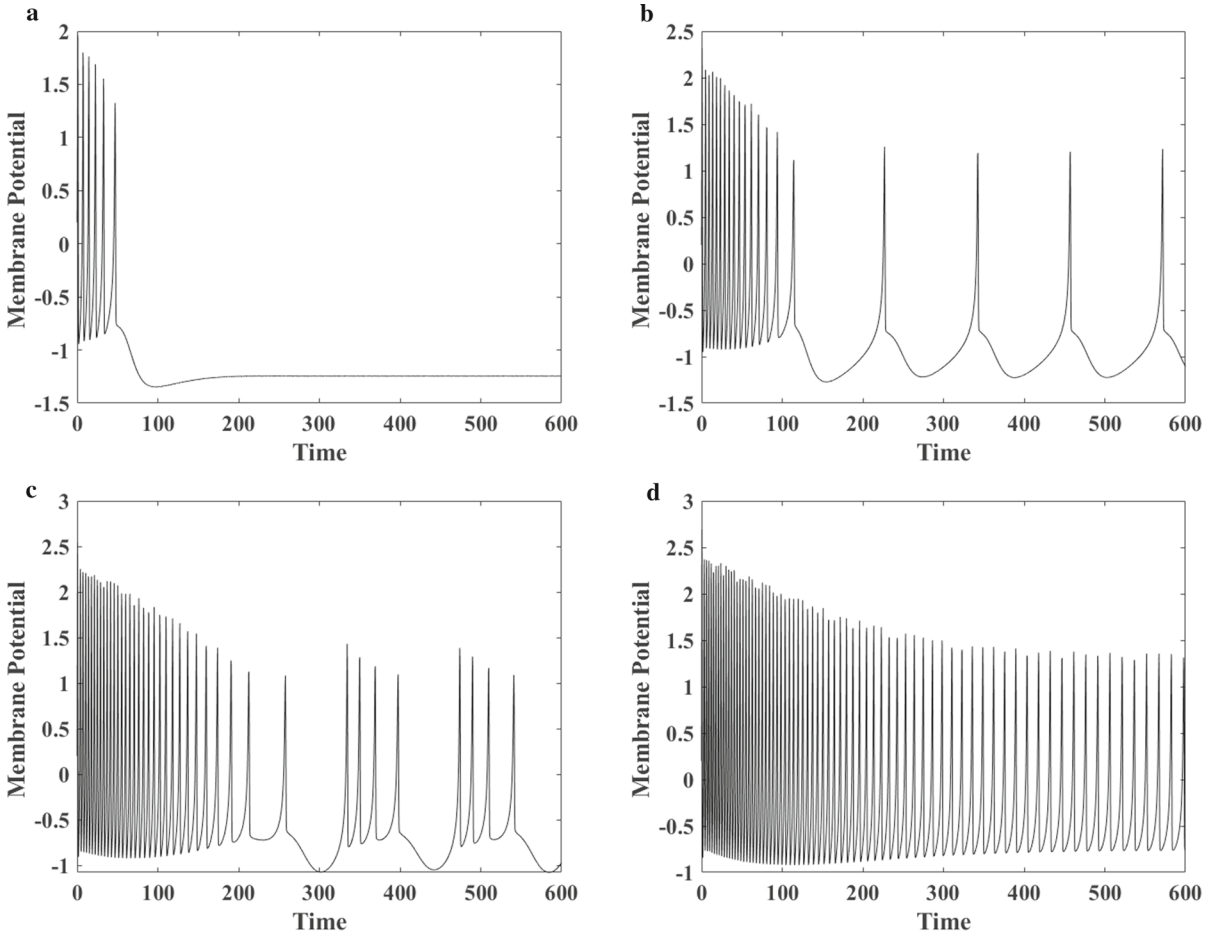

Fig. 3 Dynamics of the membrane potential of single neuron (Eq. 2) for **a** $I_{\text{ext}} = 1.0$, **b** $I_{\text{ext}} = 2.2$, **c** $I_{\text{ext}} = 3.4$ and **d** $I_{\text{ext}} = 4.5$, in parameters $a = 1, b = 3, c = 1d = 5, k = 1, r = 0.006, s = 4, k_1 = 1, k_2 = 0.5, \alpha = 0.1, \beta = 0.02$ and initial conditions (0.2, 0.5, 0.1, 0.1)

of the feedback is added to the $\dot{x}$, which presents the variations of voltage.

To design a voltage coupling, the following equations are presented:

$$\begin{aligned}
\text{neuron 1}: &\begin{cases} \dot{x_1} = y_1 - ax_1^3 + bx_1^2 - z_1 + I_{\text{ext}} - k_1\rho(\varphi_1)x_1 \\ -(\varepsilon + \eta(t))(x_1 - x_2) \\ \dot{y_1} = c - dx_1^2 - y_1 \\ \dot{z_1} = r[s(x_1 - x_0) - z_1] \\ \dot{\varphi_1} = kx_1 - k_2\varphi_1 \end{cases} \\
\text{neuron 2}: &\begin{cases} \dot{x_2} = y_2 - ax_2^3 + bx_2^2 - z_2 + I_{\text{ext}} - k_1\rho(\varphi_2)x_2 \\ -(\varepsilon + \eta(t))(x_2 - x_1) \\ \dot{y_2} = c - dx_2^2 - y_2 \\ \dot{z_2} = r[s(x_2 - x_0) - z_2] \\ \dot{\varphi_2} = kx_2 - k_2\varphi_2 \end{cases}
\end{aligned} \tag{3}$$

Indexes 1 and 2 are related to the first and second neurons. The effect of two neurons on each other can be changed by varying the coupling parameter. Parameter ε indicates the diffusive coupling strength between two neurons. Also, the effect of the neurons on each other can be different. $\eta(t)$ denotes any random noise in the model, which is ignored here. It is assumed that the information from the presynaptic neuron is transmitted to the postsynaptic one. The value $x_i - x_j$ $(i, j \in \{1, 2\})$ is taken to represent the voltage synaptic effect to the membrane potential [26].

To see the dynamics of the interactive neurons, we compare the state of the coupled neurons in parameters $k_1 = 1$, $k_2 = 05$, $\alpha = 0.1$, and $\beta = 0.02$. Similar to the single neuron study (Fig. 3), in Fig. 4,

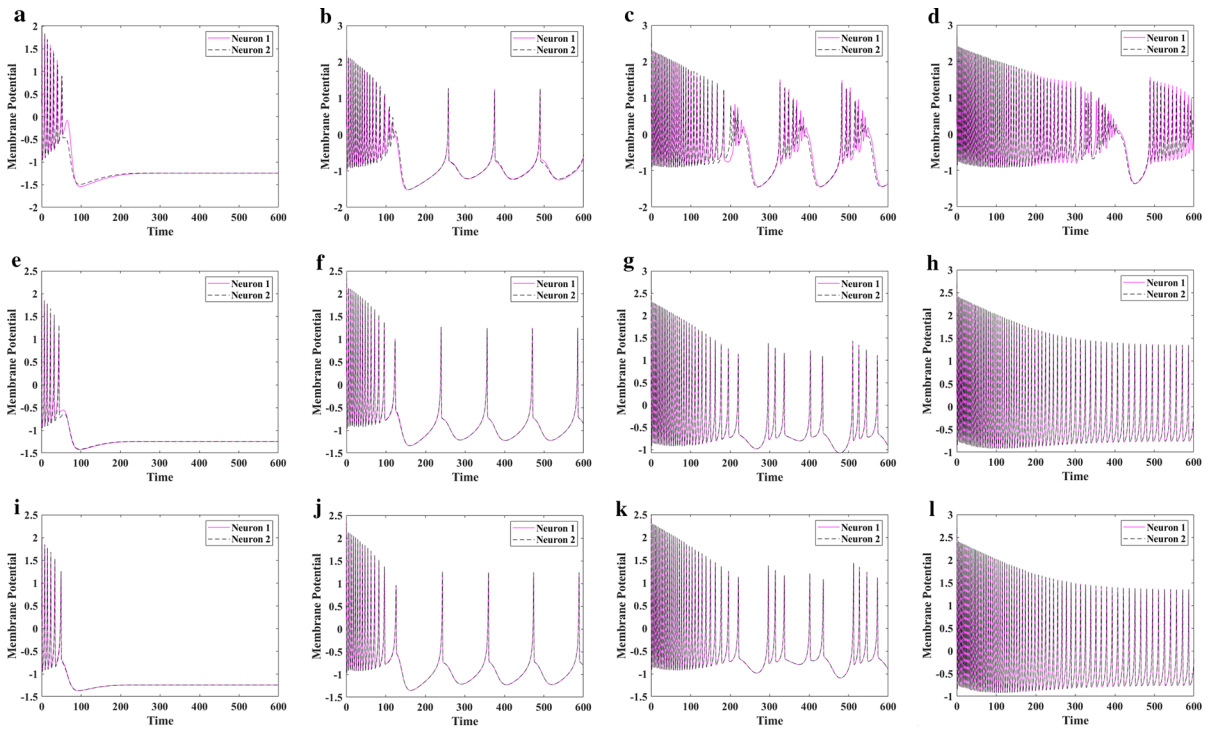

Fig. 4 Dynamics of membrane potential of two electrically coupled neurons (Eq. 3) (the pink is the response of the first neuron, and the black is the response of the second neuron) with initial conditions (0.2, 0.5, 0.1, 0.1) and (0.3, 0.8, 0.2, 0.0), in four different current forces: **a**, **e**, **i** $I_{\text{ext}} = 1.0$, **b**, **f**, **j** $I_{\text{ext}} = 2.2$; **c**, **g**, **k** $I_{\text{ext}} = 3.4$; **d**, **h**, **l** $I_{\text{ext}} = 4.5$; and by changing the coupling parameters; (the first row: $\varepsilon = 0.15$; the second row: $\varepsilon = 0.5$; and the third row: $\varepsilon = 0.75$). (Color figure online)

four different values of current force are studied as $I_{\text{ext}} = 1.0$, $I_{\text{ext}} = 2.2$, $I_{\text{ext}} = 3.4$, and $I_{\text{ext}} = 4.5$. The coupling strength is an important parameter. So, three different values of the strength are assumed as $\varepsilon = 0.15$, $\varepsilon = 0.5$, and $\varepsilon = 0.75$. All stimulations are done with initial conditions (0.2, 0.5, 0.1, 0.1) and (0.3, 0.8, 0.2, 0.0), for the first and second neurons; however, the dynamics of coupled neurons are not sensitive to initial conditions. In Fig. 4, pink patterns are related to the first neuron, and the black ones are related to the second neuron. Figure 4 shows that for lower coupling strengths, the possibility of exhibiting different dynamics is more than the cases with higher coupling values. The cases with higher coupling strength are more like the single-cell mode. To see the variety of dynamics of membrane potential in the coupled neurons with increasing external current, some bifurcation diagrams with $\varepsilon = 0.15$ are plotted in Fig. 5. According to this figure, by increasing the current force, the dynamic of steady-state changes from burst to intermittent or chaotic bursting state and then turns back to fast-spiking. The dynamics of the two neurons are the same.

To investigate the dynamics of the coupled neurons comprehensively, the time series of the two neurons are studied by considering periodic external force. It is assumed that $I_{\text{ext}} = Acos(\omega t)$. The numerical results of changing the amplitude and frequency of the current force show various dynamics of spike and burst (see Figs. 6 and 7). In Fig. 6b, after initial burst, a phasic spiking is observed, which means that the neuron has a single spike and enters into a state of inactivity despite stimulation. The trend of changing the dynamics in the case of the periodic current force is the same as applying the constant current force, but its dynamics are slower. By increasing the coupling strength, membrane potentials of two neurons become closer. Changing the amplitude of the external current in Fig. 7 shows that by increasing the frequency of external force, spikes arise in the top of sinusoidal external current.

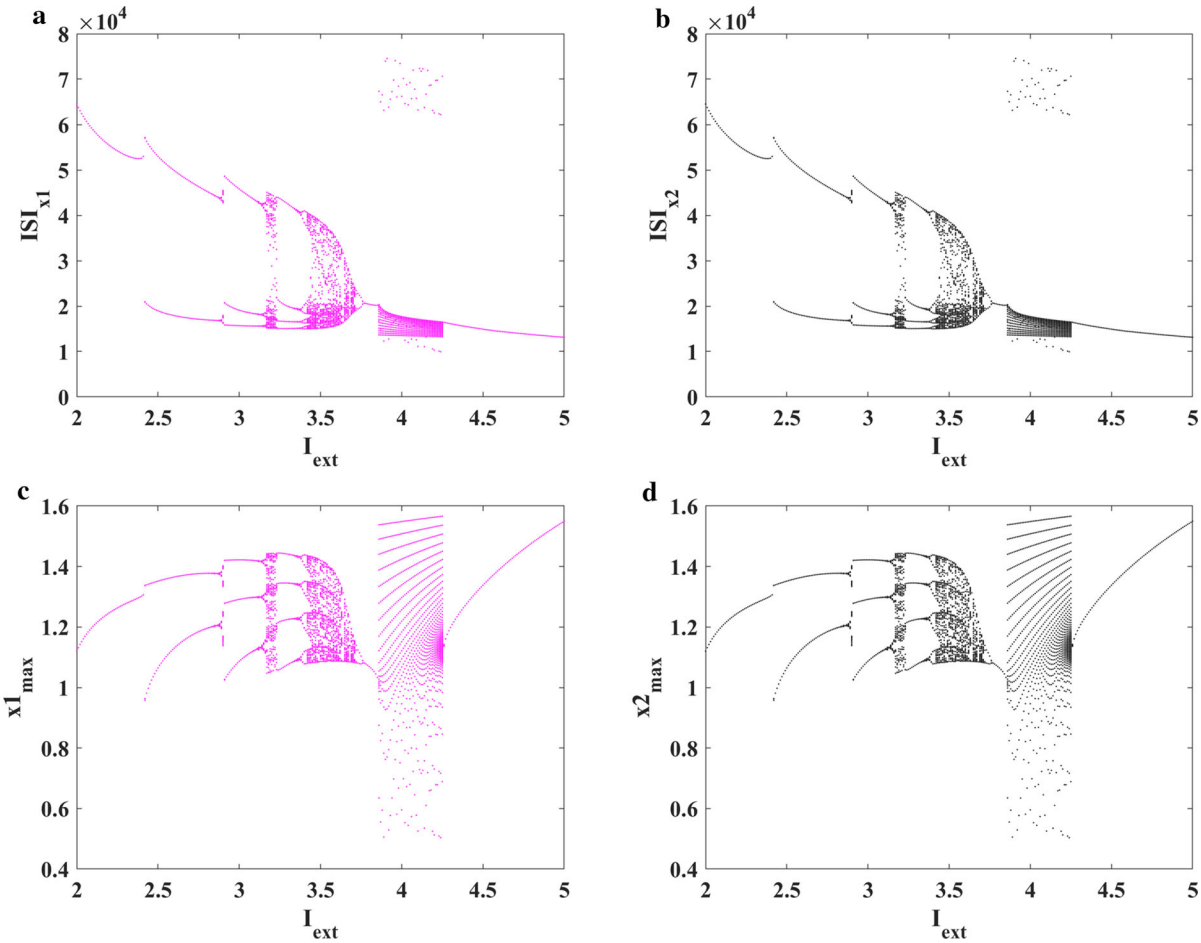

Fig. 5 Bifurcation diagram of the electrically coupled neurons (Eq. 3) with respect to the external current force I_{ext} by using constant initial conditions $(0.2, 0.5, 0.1, 0.1)$ and $(0.3, 0.8, 0.2, 0.0)$. **a** ISIs of the first neuron; **b** ISIs of the second neuron; **c** peak values of the first neuron; and **d** peak values of the second neuron; the parameters are $a = 1, b = 3, c = 1, d = 5, k = 1, r = 0.006, s = 4, k_1 = 1, k_2 = 0.5, \alpha = 0.1, \beta = 0.02, \varepsilon = 0.15$

3.2 Chemical synaptic coupling

Chemical synapses are more frequent than electrical ones in the gap junction. To better model chemical synaptic currents, the transition's dynamic of neurotransmitters is added to the equations. The modeling methods of references [49,52] have considered the chemical coupling bidirectional. We add the induction of the electromagnetic field into them and investigate their dynamics. To investigate this coupling, a model based on physiological properties should be described in the first step. There are many methods to model such interaction [26,49,52,53].

The following equations are presented based on Abarbanel et al. model [49] by adding the effect of the magnetic field.

$$
\begin{aligned}
\text{neuron 1}: &\begin{cases}
\dot{x_1} = y_1 - ax_1^3 + bx_1^2 - z_1 + I_{\text{ext}} - k_1\rho(\varphi_1)x_1 \\
\quad -(\varepsilon + \eta(t))(x_1(t) + V_c)\theta(x_2(t-\tau_c) - X) \\
\dot{y_1} = c - dx_1^2 - y_1 \\
\dot{z_1} = r[s(x_1 - x_0) - z_1] \\
\dot{\varphi_1} = kx_1 - k_2\varphi_1
\end{cases} \\
\text{neuron 2}: &\begin{cases}
\dot{x_2} = y_2 - ax_2^3 + bx_2^2 - z_2 + I_{\text{ext}} - k_1\rho(\varphi_2)x_2 \\
\quad -(\varepsilon + \eta(t))(x_2(t) + V_c)\theta(x_1(t-\tau_c) - X) \\
\dot{y_2} = c - dx_2^2 - y_2 \\
\dot{z_2} = r[s(x_2 - x_0) - z_2] \\
\dot{\varphi_2} = kx_2 - k_2\varphi_2
\end{cases}
\end{aligned}
\tag{4}
$$

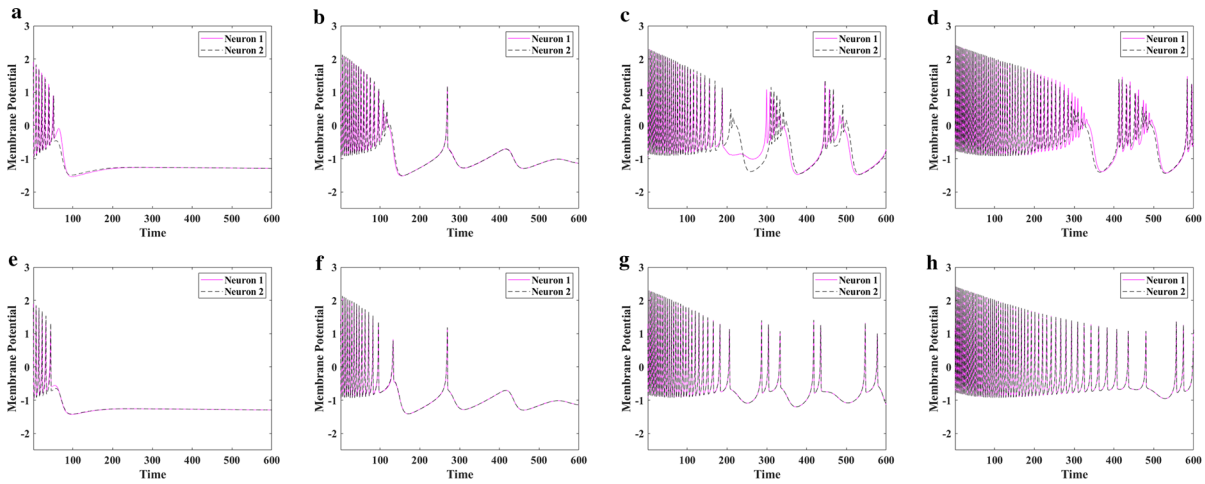

Fig. 6 Dynamics of membrane potential of the electrically coupled neurons (Eq. 3) (the pink is the response of the first neuron, and the black is the response of the second neuron) with initial conditions $(0.2, 0.5, 0.1, 0.1)$ and $(0.3, 0.8, 0.2, 0.0)$ in four different intensities of periodic force ($I_{\text{ext}} = A\cos(\omega t)$ and $\omega = 0.001$) **a**, **e** $A = 1.0$; **b**, **f** $A = 2.2$; **c**, **g** $A = 3.4$; **d**, **h** $A = 4.5$ by changing coupling parameters; the first row: $\varepsilon = 0.15$ and the second row: $\varepsilon = 0.5$. (Color figure online)

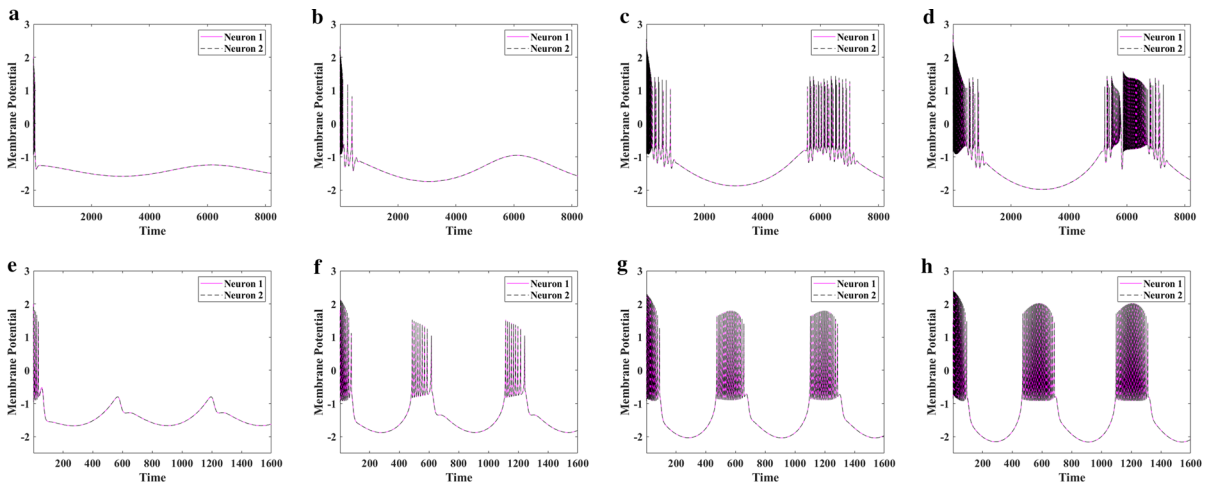

Fig. 7 Dynamics of membrane potential of the electrically coupled neurons (Eq. 3) (the pink is the response of the first neuron, and the black is the response of the second neuron) with initial conditions $(0.2, 0.5, 0.1, 0.1)$ and $(0.3, 0.8, 0.2, 0.0)$ in four different intensities of periodic force ($I_{\text{ext}} = A\cos(\omega t)$ and $\varepsilon = 0.75$) and by changing the current parameters, **a**, **e** $A = 1.0$; **b**, **f** $A = 2.2$; **c**, **g** $A = 3.4$; **d**, **h** $A = 4.5$; the first row: $\omega = 0.001$ and the second row: $\omega = 0.01$. (Color figure online)

In this model, $\theta(t)$ is the activation function. This function is considered to be Heaviside, which is a discontinuous function. In the chemical coupling, impulse transmission occurs through neurotransmitters with a short time delay τ_c [54]. By adding the term $x_i(t - \tau_c)$, the degree of freedom in this model goes to infinity, since the dimension of delayed differential equations is infinite. Parameter X is the threshold value. The membrane potential of the second neuron must reach this value to activate the coupling. If the voltages do not reach the threshold, then the coupling term goes to zero. V_c is the reverse potential, which shows the magnitude of response in the interaction. The threshold of potential is considered $X = 0.85$. $V_c > 1$ is a reverse potential. By choosing $V_c > 1$, inhibitory coupling happens [49]. Figure 8 shows the dynamics of neurons by using $V_c = 1.4$ (inhibitory coupling). By increasing the strength of coupling in a specific and limited domain, related

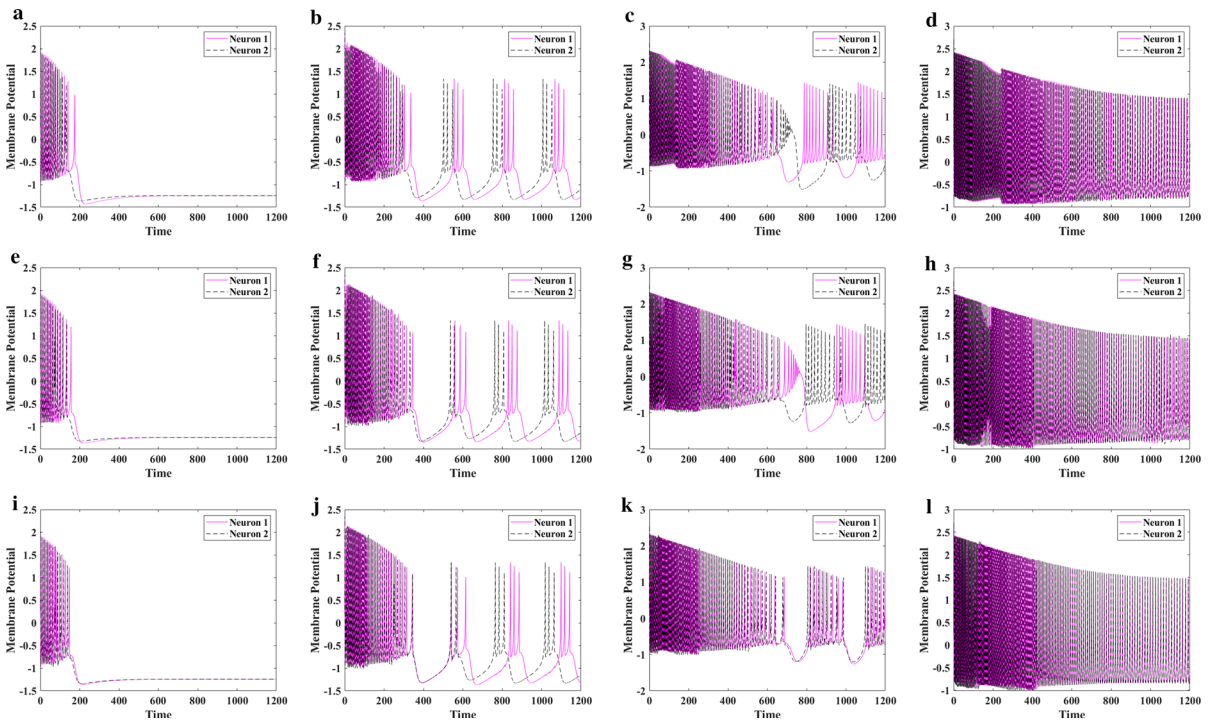

Fig. 8 Dynamics of the membrane potential of the chemically coupled neurons (Eq. 4) (the pink is the response of the first neuron, and the black is the response of the second neuron) with initial conditions $(0.2, 0.5, 0.1, 0.1)$ and $(0.3, 0.8, 0.2, 0.0)$ in four different currents and by changing coupling parameters. The first row: $\varepsilon = 0.15$; the second row: $\varepsilon = 0.5$; and the third row: $\varepsilon = 0.75$. **a**, **e**, **i** $I_{\text{ext}} = 1.0$; **b**, **f**, **j** $I_{\text{ext}} = 2.2$; **c**, **g**, **k** $I_{\text{ext}} = 3.4$; d, h, l) $I_{\text{ext}} = 4.5$; the parameters are $r = 0.0021$, $\tau_c = 4$, $X = 0.85$, $V_c = 1.4$. (Color figure online)

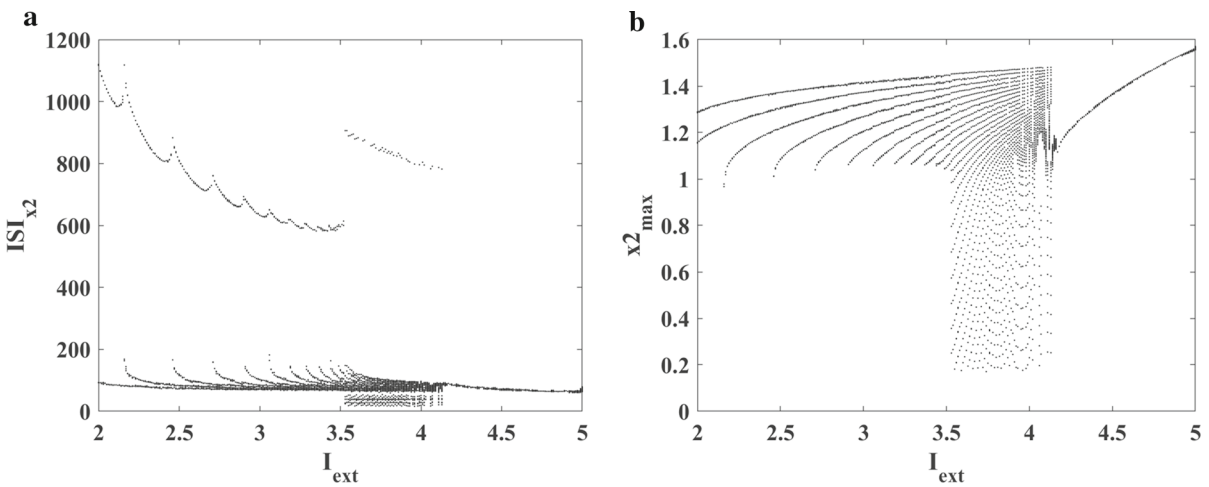

Fig. 9 Bifurcation diagram of chemically coupled neurons (Eq. 4) using constant initial conditions $(0.2, 0.5, 0.1, 0.1)$ and $(0.3, 0.8, 0.2, 0.0)$ with respect to changing external force I_{ext}. **a** ISIs of the second neuron; and **b** peak values of the second neuron, at $\tau_c = 4$, $X = 0.85$, $V_c = 1.4$, $\varepsilon = 0.15$

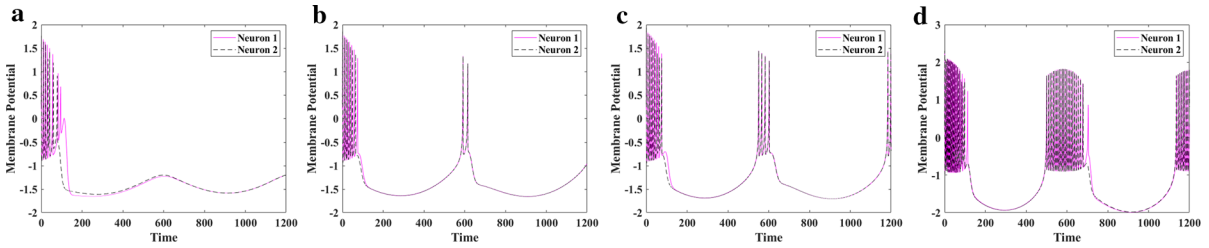

Fig. 10 Dynamics of membrane potential of the chemically coupled neurons (Eq. 4) (the pink is the response of the first neuron, and the black is the response of the second neuron) with initial conditions (0.2, 0.5, 0.1, 0.1) and (0.3, 0.8, 0.2, 0.0) in four different intensities of periodic current ($I_{\text{ext}} = A\cos(\omega t)$ and $\omega = 0.01$), in coupling parameter $\varepsilon = 0.15$, **a** $A = 0.4$; **b** $A = 0.58$; **c** $A = 0.75$; and **d** $A = 2$. (Color figure online)

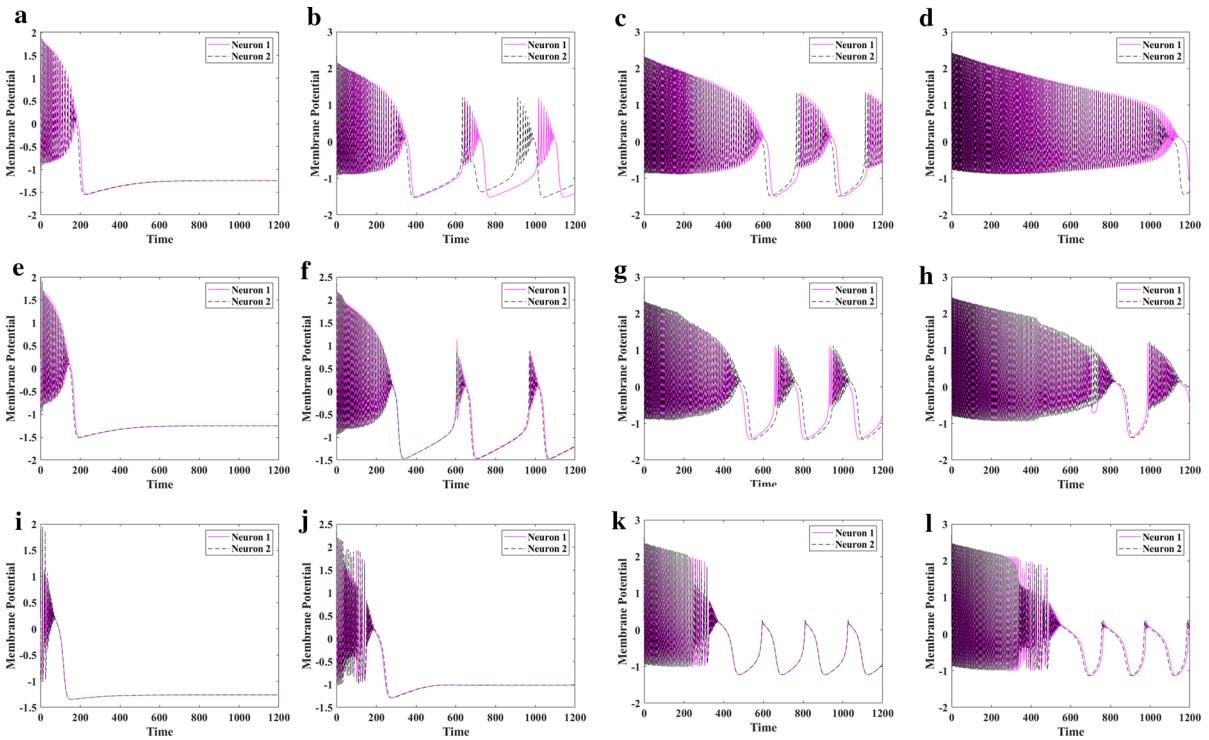

Fig. 11 Dynamics of membrane potential of two chemically coupled neurons (Eq. 5) (the pink is the response of the first neuron, and the black is the response of the second neuron) with initial conditions (0.2, 0.5, 0.1, 0.1) and (0.3, 0.8, 0.2, 0.0) in four different currents and by changing coupling parameters. The first row: $\varepsilon = 0.05$; the second row: $\varepsilon = 0.15$; and the third row: $\varepsilon = 0.5$. **a**, **e**, **i** $I_{\text{ext}} = 1.0$; **b**, **f**, **j** $I_{\text{ext}} = 2.2$; **c**, **g**, **k** $I_{\text{ext}} = 3.4$; **d**, **h**, **l** $I_{\text{ext}} = 4.5$; the parameters are $r = 0.0021, X = 0.85, V_c = 1.4, \sigma = 0.01$. (Color figure online)

to the external current force, neurons oscillate out-of-phase (anti-phasic synchronization). By increasing the current, one neuron lags from the other one. In parts (c) and (g) of Fig. 8, asynchronization occurs.

In Fig. 9, the bifurcation diagram of the coupled neurons in small strength of coupling ($\varepsilon = 0.15$) is plotted. Since the dynamics of the two neurons are the same, just the bifurcation diagram of the second neuron is sketched. By increasing the current force, the dynamics of steady state are changed. There are various types of bursting [54,55]. According to Fig. 9, the output of membrane potential is burst when the current force is larger than 2. In the interval $I_{\text{ext}} \in [3.4, 4.15]$, the pattern of membrane potential changes to tonic bursting or chattering (like square wave bursting; Fig. 8c). By increasing the current to larger values than 4.15, the

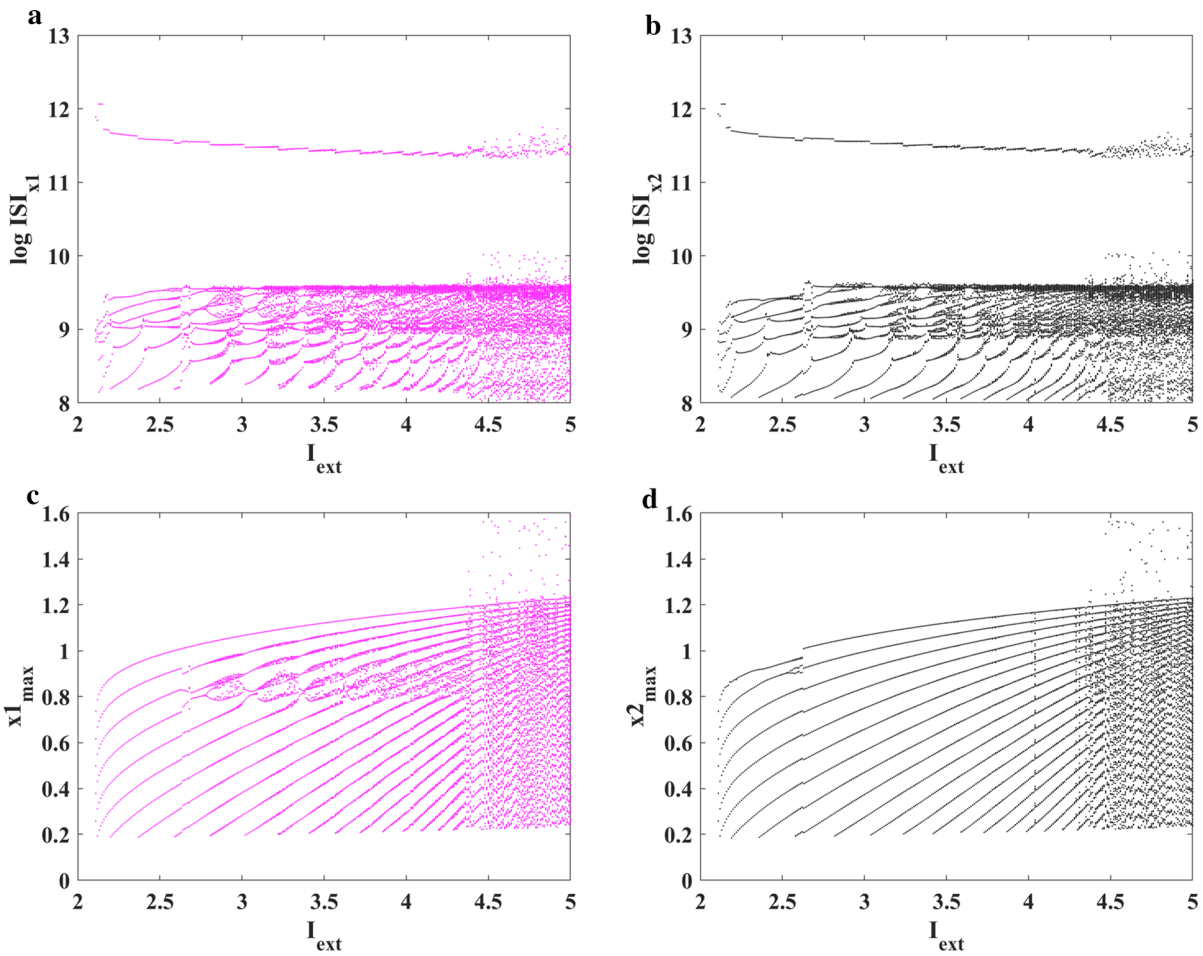

Fig. 12 Bifurcation diagram of chemically coupled neurons (Eq. 5) with constant initial conditions $(0.2, 0.5, 0.1, 0.1)$ and $(0.3, 0.8, 0.2, 0.0)$ with respect to the external current I_{ext} . **a** Logarithm of ISIs for the first neuron; **b** logarithm of ISIs for the second neuron; **c** maximum peaks for the first neuron; and **d** maximum peaks for the second neuron in $r = 0.0021$, $X = 0.85$, $V_c = 1.4$, $\varepsilon = 0.15$, $\sigma = 0.01$

only regular fast-spiking pattern is observed. In comparison with the dynamics of electrically coupled neurons, the variations are the same, but in the chemical coupling, the two neurons are not synchronized in any cases.

To investigate the periodic external force, the sinusoidal current injection is assumed, and the numerical results are presented in Fig. 10. It can be seen that in this current injection, two neurons are forced to synchronize, and even in smaller currents, burst dynamics are observed. It can be concluded that sinusoidal stimulation has a more significant effect on the chemical coupling.

In the chemical coupling, the activation function can be sigmoid [56]. In reality, a complex behavior such as activation of a neuron by reaching the threshold is not a step function. In the improvement in the model, $1/(1+\exp((V_i - X)/\sigma))$ mimics the activation function [53]. The chemical coupling by the sigmoid activation function is proposed in Eq. 5:

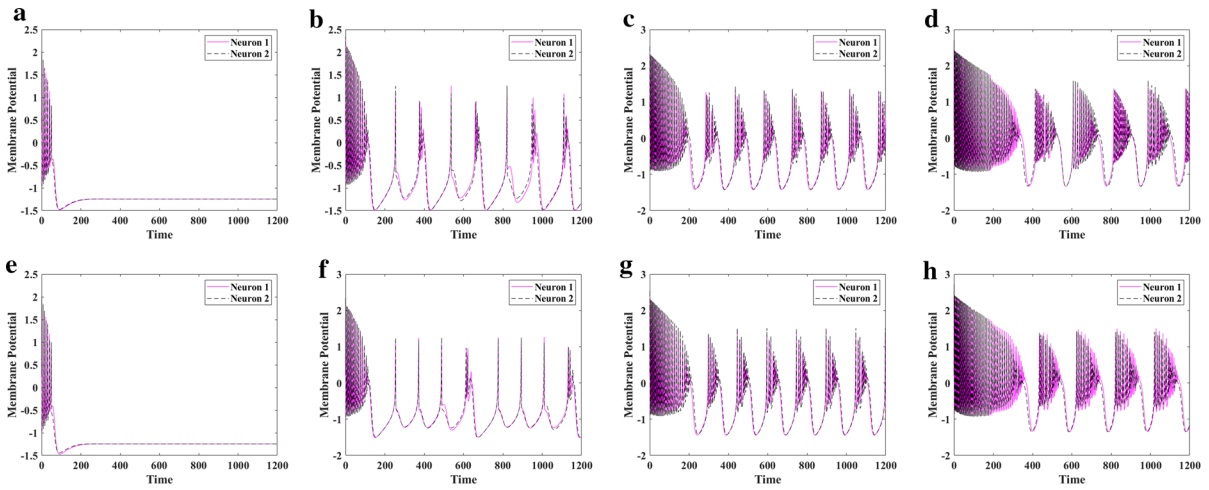

Fig. 13 Dynamics of the membrane potential of the mixed-coupled neurons (Eq. 6) (the pink is the response of the first neuron, and the black is the response of the second neuron) with initial conditions $(0.2, 0.5, 0.1, 0.1)$ and $(0.3, 0.8, 0.2, 0.0)$ in four different currents and with changing coupling parameters. The first row: $\varepsilon_i = 0.05$ and $\varepsilon_e = 0.1$, and the second row: $\varepsilon_i = 0.02$ and $\varepsilon_e = 0.15$. **a**, **e** $I_{\text{ext}} = 1.0$; **b**, **f** $I_{\text{ext}} = 2.2$; **c**, **g** $I_{\text{ext}} = 3.4$; **d**, **h** $I_{\text{ext}} = 4.5$. (Color figure online)

$$
\begin{aligned}
\text{neuron 1}: &\begin{cases}
\dot{x_1} = y_1 - ax_1^3 + bx_1^2 - z_1 + I_{\text{ext}} - k_1\rho(\varphi_1)x_1 \\
-(\varepsilon + \eta(t))(\frac{x_1+V_c}{1+exp(\frac{x_2-X}{\sigma})}) \\
\dot{y_1} = c - dx_1^2 - y_1 \\
\dot{z_1} = r[s(x_1 - x_0) - z_1] \\
\dot{\varphi_1} = kx_1 - k_2\varphi_1
\end{cases} \\
\text{neuron 2}: &\begin{cases}
\dot{x_2} = y_2 - ax_2^3 + bx_2^2 - z_2 + I_{\text{ext}} - k_1\rho(\varphi_2)x_2 \\
-(\varepsilon + \eta(t))(\frac{x_2+V_c}{1+exp(\frac{x_1-X}{\sigma})}) \\
\dot{y_2} = c - dx_2^2 - y_2 \\
\dot{z_2} = r[s(x_2 - x_0) - z_2] \\
\dot{\varphi_2} = kx_2 - k_2\varphi_2
\end{cases}
\end{aligned}
\tag{5}
$$

In this model, simulations are done by neglecting the effect of time delay and using the sigmoid function as the activation function. In Fig. 11, it can be seen that by using Eq. 5 the synchronizations of neurons are more than the delayed equations. Also, there is a lag between responses, without any delay factor in the equations. This figure shows that spike responses disappear as the strength of coupling increases. It is also observed that in most of the parameters, the response pattern is triangle bursting.

In this case, the bifurcation diagrams of the two neurons are different. To better show the details of ISIs bifurcation, it is plotted in logarithm scale in Fig. 12.

3.3 Electrochemical coupling

In this case, it is assumed that the two neurons (which are chemically coupled) are also electrically dependent because of their position. These dynamics exist for many cells located in the cortex and small neuronal systems [12–14]. In this case, the coupling is considered inhibitory. Some models study the chemical couplings inhibitory or excitatory [49], while some others only consider the inhibitory chemical couplings [52,53]. In this paper, we have used both types of models (Eqs. 4 and 5). To compare these two models, we have focused on the inhibitory coupling. Then, it is mixed with electrical coupling and will generate the model of electrochemical coupling. The description of mixed coupling has been considered in [52,57]. In this paper, the electrochemical coupling by considering the effect of electromagnetic field injection is studied. The model of the electrochemical coupling under the electromagnetic field is shown in the following equation:

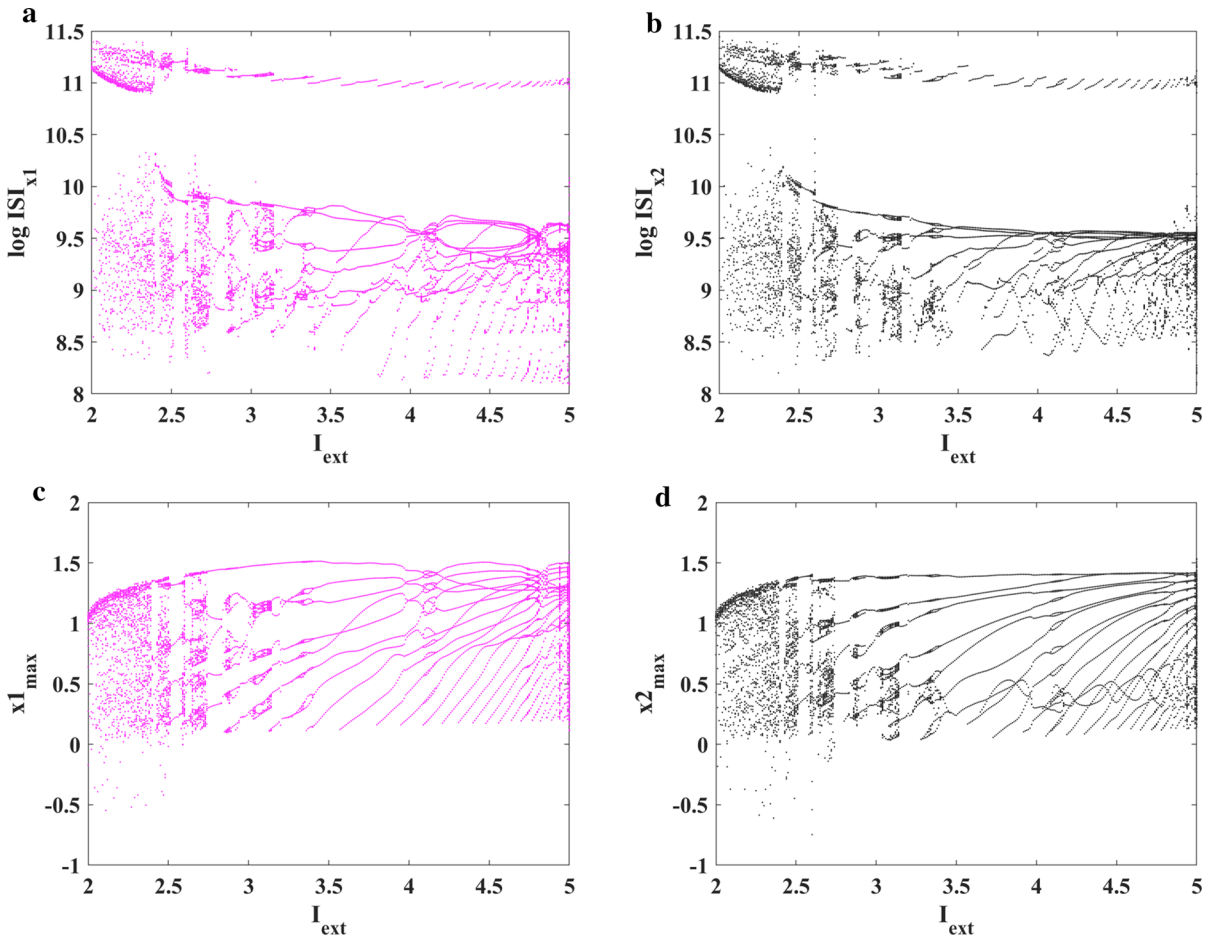

Fig. 14 Bifurcation diagram of the mixed-coupled neurons (Eq. 6) with respect to the external current I_{ext} by using constant initial conditions $(0.2, 0.5, 0.1, 0.1)$ and $(0.3, 0.8, 0.2, 0.0)$. **a** Logarithm of ISIs for the first neuron; **b** logarithm of ISIs for the second neuron; **c** maximum peaks of the first neuron; and **d** maximum peaks of the second neuron in $X = 0.85$, $V_c = 1.4$, $\sigma = 0.01$, $\varepsilon_i = 0.02$, and $\varepsilon_e = 0.15$

$$
\begin{aligned}
\text{neuron 1}: &\begin{cases}
\dot{x_1} = y_1 - ax_1^3 + bx_1^2 - z_1 + I_{\text{ext}} - k_1\rho(\varphi_1)x_1 \\
\quad -\varepsilon_i\left(\frac{x_1+V_c}{1+exp(\frac{x_2-X}{\sigma})}\right) - \varepsilon_e(x_1 - x_2) \\
\dot{y_1} = c - dx_1^2 - y_1 \\
\dot{z_1} = r[s(x_1 - x_0) - z_1] \\
\dot{\varphi_1} = kx_1 - k_2\varphi_1
\end{cases} \\
\text{neuron 2}: &\begin{cases}
\dot{x_2} = y_2 - ax_2^3 + bx_2^2 - z_2 + I_{\text{ext}} - k_1\rho(\varphi_2)x_2 \\
\quad -\varepsilon_i\left(\frac{x_2+V_c}{1+exp(\frac{x_1-X}{\sigma})}\right) - \varepsilon_e(x_2 - x_1) \\
\dot{y_2} = c - dx_2^2 - y_2 \\
\dot{z_2} = r[s(x_2 - x_0) - z_2] \\
\dot{\varphi_2} = kx_2 - k_2\varphi_2
\end{cases}
\end{aligned}
\tag{6}
$$

In this model (Eq. 6), ε_i and ε_e are the strength of chemical and electrical coupling, and the sigmoid function is chosen as an activation function in chemical coupling. Dynamical properties of the coupled neurons under electrochemical coupling are investigated in the following of this subsection. In this case, two parameters should be studied: the strength of chemical coupling and the strength of electrical coupling. Figure 13 shows the dynamics of coupled neurons in electrochemical coupling. A comparison of this coupling with the previous ones determines that the number of spikes in electrochemical coupling is larger than that of the previous cases in the same interval of time. So, the dynamics of neurons in this coupling is faster. Figure 13b, f represents that in this coupling, there are some cases in which a mixture of spike and burst exists.

Figure 14 shows the bifurcation diagram of the electrochemical coupling. The dynamics of the two neurons

are different. To better show the details of ISIs bifurcations, the logarithmic scale of the values is plotted. In this coupling, the bifurcation diagram is richer than the previous ones. By increasing the external force, chaotic dynamics emerge. In some intervals, the periodic windows can be seen. So, it can be concluded that the neurons with the potency of coupling in both electrical and chemical form can show various dynamics in each stimulation.

4 Conclusion

In this paper, the effect of various types of couplings on the dynamical behavior of the neurons was studied. For this purpose, two Hindmarsh–Rose neurons under the magnetic field were considered in three different cases of electrical, chemical, and electrochemical coupling. In the first case, in which the coupling was electrical, the impacts of variations of current forces and the coupling strength were studied. Also, the effect of the sinusoidal current force was investigated. It was shown that in the case of the sinusoidal current force, the membrane potential has the trend of the stimulus. In the second case, for the chemical coupling two activation functions of the Heaviside and sigmoid were considered. The sigmoid activation function was near to reality in concept, and its results were more complicated than the Heaviside activation function. Moreover, the results of the sigmoid activation function showed that the membrane potentials of two neurons have a lag, even without any latency term in their equations. The third studied coupling was the mixture of the previous ones, which was called electrochemical. The sigmoid activation function was used in this coupling. The results showed that in the same time interval, the number of spikes of this case was larger than the other coupling types. Also, its bifurcation diagrams have presented richer dynamics. So, it can be concluded that the mixture of electrical and chemical couplings can show richer variety of dynamical behaviors.

Acknowledgements This work was partially supported by Iran Science Elites Federation (Grant No. M-97171). Matjaž Perc was supported by the Slovenian Research Agency (Grant Nos. J4-9302, J1-9112, and P1-0403).

Compliance with ethical standards

Conflict of interest The authors declare no conflict of interest.

References

1. Levi-Montalcini, R.: The nerve growth factor: its role in growth, differentiation and function of the sympathetic adrenergic neuron. In: Corner, M.A., Swaab, D.F. (eds.) Progress in Brain Research, vol. 45, pp. 235–258. Elsevier (1976). https://doi.org/10.1016/S0079-6123(08)60993-0
2. Koch, C., Segev, I.: The role of single neurons in information processing. Nat. Neurosci. **3**(11s), 1171 (2000)
3. Lisman, J.E.: Bursts as a unit of neural information: making unreliable synapses reliable. Trends Neurosci. **20**(1), 38 (1997)
4. Hikosaka, R., Takahashi, M., Takahata, M.: Variability and invariability in the structure of an identified nonspiking interneuron of crayfish as revealed by three-dimensional morphometry. Zool. Sci. **13**(1), 69 (1996)
5. Matthews, G.: Vesicle fiesta at the synapse. Nature **406**(6798), 835 (2000)
6. Ovsepian, S.V., Vesselkin, N.P.: Wiring prior to firing: the evolutionary rise of electrical and chemical modes of synaptic transmission. Rev. Neurosci. **25**(6), 821 (2014)
7. Keener, J.P., Sneyd, J.: Mathematical Physiology, vol. 1. Springer, Berlin (1998)
8. Schmitz, F., Königstorfer, A., Südhof, T.C.: RIBEYE, a component of synaptic ribbons: a protein's journey through evolution provides insight into synaptic ribbon function. Neuron **28**(3), 857 (2000)
9. Shefchyk, S., Jordan, L.: Excitatory and inhibitory postsynaptic potentials in alpha-motoneurons produced during fictive locomotion by stimulation of the mesencephalic locomotor region. J. Neurophysiol. **53**(6), 1345 (1985)
10. Belousov, A.B., Fontes, J.D.: Neuronal gap junctions: making and breaking connections during development and injury. Trends Neurosci. **36**(4), 227 (2013)
11. Eugenin, E.A., Basilio, D., Sáez, J.C., Orellana, J.A., Raine, C.S., Bukauskas, F., Bennett, M.V., Berman, J.W.: The role of gap junction channels during physiologic and pathologic conditions of the human central nervous system. J. Neuroimmune Pharmacol. **7**(3), 499 (2012)
12. Rash, J.E., Dillman, R.K., Bilhartz, B.L., Duffy, H.S., Whalen, L.R., Yasumura, T.: Mixed synapses discovered and mapped throughout mammalian spinal cord. Proc. Natl. Acad. Sci. **93**(9), 4235 (1996)
13. Sotelo, C., Korn, H.: Morphological correlates of electrical and other interactions through low-resistance pathways between neurons of the vertebrate central nervous system. In: Bourne, G.H., Danielli, J.F., Jeon, K.W. (eds.) International Review of Cytology, vol. 55, pp. 67–107. Academic Press (1978). https://doi.org/10.1016/S0074-7696(08)61887-2
14. Pereda, A.E.: Electrical synapses and their functional interactions with chemical synapses. Nat. Rev. Neurosci. **15**(4), 250 (2014)
15. Lindsay, K., Ogden, J., Halliday, D., Rosenberg, J.: An introduction to the principles of neuronal modelling. In: *Modern techniques in neuroscience research* (Springer), pp. 213–306 (1999)
16. Hodgkin, A.L., Huxley, A.F.: A quantitative description of membrane current and its application to conduction and excitation in nerve. J. Physiol. **117**(4), 500 (1952)

17. Nagumo, J., Arimoto, S., Yoshizawa, S.: An active pulse transmission line simulating nerve axon. Proc. IRE **50**(10), 2061 (1962)
18. FitzHugh, R.: Mathematical models of threshold phenomena in the nerve membrane. Bull. Math. Biol. **17**(4), 257 (1955)
19. Izhikevich, E.M., Trans, I.E.E.E.: Which model to use for cortical spiking neurons? Neural Netw. **15**(5), 1063 (2004)
20. Hindmarsh, J.L., Rose, R.: A model of neuronal bursting using three coupled first order differential equations. Proc. R. Soc. Lond. **221**(1222), 87 (1984)
21. Innocenti, G., Morelli, A., Genesio, R., Torcini, A.: Dynamical phases of the Hindmarsh-Rose neuronal model: studies of the transition from bursting to spiking chaos. Chaos **17**(4), 043128 (2007)
22. Hindmarsh, J., Cornelius, P.: The development of the Hindmarsh–Rose model for bursting. In: Coombes, S., Bressloff, P.C. (eds.) Bursting: The Genesis of Rhythm in the Nervous System, pp. 3–18. World Scientific (2005). https://doi.org/10.1142/9789812703231_0001
23. Lv, M., Ma, J.: Multiple modes of electrical activities in a new neuron model under electromagnetic radiation. Neurocomputing **205**, 375 (2016)
24. Bao, B., Hu, A., Bao, H., Xu, Q., Chen, M., Wu, H.: Three-dimensional memristive Hindmarsh-Rose neuron model with hidden coexisting asymmetric behaviors. Complexity **2018**, 1–11 (2018)
25. Tang, K., Wang, Z., Shi, X.: Electrical activity in a time-delay four-variable neuron model under electromagnetic induction. Front. Comput. Neurosci. **11**, 105 (2017)
26. Mostaghimi, S., Nazarimehr, F., Jafari, S., Ma, J.: Chemical and electrical synapse-modulated dynamical properties of coupled neurons under magnetic flow. Appl. Math. Comput. **348**, 42 (2019)
27. Azevedo, F.A., Carvalho, L.R., Grinberg, L.T., Farfel, J.M., Ferretti, R.E., Leite, R.E., Filho, W.J., Lent, R., Herculano-Houzel, S.: Equal numbers of neuronal and nonneuronal cells make the human brain an isometrically scaled-up primate brain. J. Comput. Neurol. **513**(5), 532 (2009)
28. Zimmer, C.: 100 trillion connections. Sci. Am. **304**(1), 58 (2011)
29. Ma, J., Wu, F., Wang, C.: Synchronization behaviors of coupled neurons under electromagnetic radiation. Int. J. Mod. Phys. B **31**(2), 1650251 (2017)
30. Zhao, Y., Sun, X., Liu, Y., Kurths, J.: Phase synchronization dynamics of coupled neurons with coupling phase in the electromagnetic field. Nonlinear Dyn. **93**(3), 1315 (2018)
31. Xu, Y., Jia, Y., Kirunda, J.B., Shen, J., Ge, M., Lu, L., Pei, Q.: Dynamic behaviors in coupled neuron system with the excitatory and inhibitory autapse under electromagnetic induction. Complexity **2018**, 1–13 (2018)
32. Rostami, Z., Jafari, S.: Defects formation and spiral waves in a network of neurons in presence of electromagnetic induction. Cognit. Neurodyn. **12**(2), 235 (2018)
33. Lv, M., Ma, J., Yao, Y., Alzahrani, F.: Synchronization and wave propagation in neuronal network under field coupling. Sci. China Technol. Sci. **62**(3), 448 (2019)
34. Ma, J., Mi, L., Zhou, P., Xu, Y., Hayat, T.: Phase synchronization between two neurons induced by coupling of electromagnetic field. Appl. Math. Comput. **307**, 321 (2017)
35. Hindmarsh, J., Rose, R.: A model of the nerve impulse using two first-order differential equations. Nature **296**(5853), 162 (1982)
36. Wang, X.J.: Genesis of bursting oscillations in the Hindmarsh-Rose model and homoclinicity to a chaotic saddle. Physica D **62**(1–4), 263 (1993)
37. Lv, M., Wang, C., Ren, G., Ma, J., Song, X.: Model of electrical activity in a neuron under magnetic flow effect. Nonlinear Dyn. **85**(3), 1479 (2016)
38. Ma, J., Tang, J.: A review for dynamics of collective behaviors of network of neurons. Sci. China Technol. Sci. **58**(12), 2038 (2015)
39. Etémé, A.S., Tabi, C.B., Mohamadou, A.: Firing and synchronization modes in neural network under magnetic stimulation. Commun. Nonlinear Sci. Numer. Simul. **72**, 432 (2019)
40. Bao, B., Liu, Z., Xu, J.: Steady periodic memristor oscillator with transient chaotic behaviours. Electron. Lett. **46**(3), 237 (2010)
41. Neumann, F.E.: General laws of induced electric strings. Ann. Phys. **143**(1), 31 (1846)
42. Ma, J., Yang, Zq, Yang, Lj, Tang, J.: A physical view of computational neurodynamics. J. Zhejiang Univ. Sci. A **20**(9), 639 (2019)
43. Rostami, Z., Jafari, S., Perc, M., Slavinec, M.: Elimination of spiral waves in excitable media by magnetic induction. Nonlinear Dyn. **94**(1), 679 (2018)
44. Reich, D.S., Mechler, F., Purpura, K.P., Victor, J.D.: Interspike intervals, receptive fields, and information encoding in primary visual cortex. J. Neurosci. **20**(5), 1964 (2000)
45. Xia, S., Qi-Shao, L.: Firing patterns and complete synchronization of coupled Hindmarsh–Rose neurons. Chin. Phys. **14**(1), 77 (2005)
46. Shuai, J.W., Durand, D.M.: Phase synchronization in two coupled chaotic neurons. Phys. Lett. A **264**(4), 289 (1999)
47. Elson, R.C., Selverston, A.I., Huerta, R., Rulkov, N.F., Rabinovich, M.I., Abarbanel, H.D.: Synchronous behavior of two coupled biological neurons. Phys. Rev. Lett. **81**(25), 5692 (1998)
48. Varona, P., Torres, J.J., Abarbanel, H.D., Rabinovich, M.I., Elson, R.C.: Dynamics of two electrically coupled chaotic neurons: experimental observations and model analysis. Biol. Cybernet. **84**(2), 91 (2001)
49. Abarbanel, H.D., Huerta, R., Rabinovich, M.I., Rulkov, N.F., Rowat, P.F., Selverston, A.I.: Synchronized action of synaptically coupled chaotic model neurons. Neural Comput. **8**(8), 1567 (1996)
50. Parastesh, F., Azarnoush, H., Jafari, S., Hatef, B., Perc, M., Repnik, R.: Synchronizability of two neurons with switching in the coupling. Appl. Math. Comput. **350**, 217 (2019)
51. Meşe, G., Richard, G., White, T.W.: Gap junctions: basic structure and function. J. Investig. Dermatol. **127**(11), 2516 (2007)
52. Huerta, R., Rabinovich, M.I., Abarbanel, H.D., Bazhenov, M.: Spike-train bifurcation scaling in two coupled chaotic neurons. Phys. Rev. E **55**(3), R2108 (1997)
53. Bazhenov, M., Huerta, R., Rabinovich, M., Sejnowski, T.: Cooperative behavior of a chain of synaptically coupled chaotic neurons. Physica D **116**(3–4), 392 (1998)
54. Lodish, H., Berk, A., Zipursky, S.L., et al.: Molecular cell biology, 4th edn. W. H. Freeman, New York (2000).

Available from: https://www.ncbi.nlm.nih.gov/books/NBK21475/
55. Izhikevich, E.M., Trans, E.E.E.: Simple model of spiking neurons. Neural Netw. **14**(6), 1569 (2003)
56. Jalili, M.: Collective behavior of interacting locally synchronized oscillations in neuronal networks. Commun. Nonlinear Sci. Numer. Simul. **17**(10), 3922 (2012)
57. Wu, Y., Xu, J., Jin, W.: Synchronous behaviors of two coupled neurons. In: Wang, J., Liao, X., Yi, Z. (eds.) Advances in Neural Networks – ISNN 2005, pp. 302–307. Springer, Berlin, Heidelberg (2005). https://doi.org/10.1007/11427391_47